

Unsupervised Domain Adaptation Using Feature Disentanglement And GCNs For Medical Image Classification

Dwarikanath Mahapatra

Inception Institute of AI, UAE

Abstract. The success of deep learning has set new benchmarks for many medical image analysis tasks. However, deep models often fail to generalize in the presence of distribution shifts between training (source) data and test (target) data. One method commonly employed to counter distribution shifts is domain adaptation: using samples from the target domain to learn to account for shifted distributions. In this work we propose an unsupervised domain adaptation approach that uses graph neural networks and, disentangled semantic and domain invariant structural features, allowing for better performance across distribution shifts. We propose an extension to swapped autoencoders to obtain more discriminative features. We test the proposed method for classification on two challenging medical image datasets with distribution shifts - multi center chest Xray images and histopathology images. Experiments show our method achieves state-of-the-art results compared to other domain adaptation methods.

Keywords: Unsupervised domain adaptation, Graph convolution networks, Camelyon17, CheXpert, NIH Xray.

1 Introduction

The success of convolutional neural networks (CNNs) has set new benchmarks for many medical image classification tasks such as diabetic retinopathy grading [27], digital pathology image classification [50,149,36,19,175,143,44,151,37,12,104] and chest X-ray images [33,177,91,92,108,111,60,59,62,119,58,135,133,132,144,53], as well as segmentation tasks [47,154,24,9,7,77,67,182,141,89,64,48,63,107]. Clinical adoption of algorithms has many challenges due to the domain shift problem: where the target dataset has different characteristics than the source dataset on which the model was trained. These differences are often a result of different image capturing protocols, parameters, devices, scanner manufacturers, etc. Since annotating samples from hospitals and domains is challenging due to scarcity of experts and the resource intensive nature of labeling, it is essential to design models from the beginning that perform consistently on images acquired from multiple domains.

Most approaches to the domain shift problem can be categorized based on the amount of data from the target domain. Fully-supervised domain adaptation

(DA) and semi-supervised DA assume availability of a large amount and a small amount of fully-labeled instances from the target domain, respectively, along with data from a source domain [157,17,146,78,155,171,112,79,38,173,82,10,80,41,13,180,103,86,106]. Unsupervised domain adaptation (UDA) techniques [16,153,166,167,74,168,85,160,159,172,170,65,116,169,115,1] use only unlabeled data from the target domain and labeled source domain data. UDA methods aim to learn a domain-invariant representation by enforcing some constraint (e.g. Maximum Mean Discrepancy [46]) that brings the latent space distributions, z , of distinct domains closer; ideally leading to more comparable performance in classification/segmentation.

Convolutional neural network (CNN) based state-of-the-art (SOTA) UDA methods often obtain impressive results but typically only enforce alignment of global domain statistics [179,93,113,140,45,110,164,165,109,121,163,61,90,139,137,138,136,55] resulting in loss of semantic class label information. Semantic transfer methods [51,152,57,176,56,54,134,128,130,131,129,125,126,120,117,127,142,114] address this by propagating class label information into deep adversarial adaptation networks. Unfortunately, it is difficult to model and integrate semantic label transfer into existing deep networks. To deal with the above limitations [52,147,148,150,20,18,124,145,72,42,71,40,34,35,1] propose a Graph Convolutional Adversarial Network (GCAN) for unsupervised domain adaptation. Graph based methods better exploit global relationship between different nodes (or samples) than CNNs and learn both global and local information beneficial for DA.

One way to address domain shift is with feature disentanglement [49] by separating latent feature representations into domain invariant (often called structure or content) and domain variant (texture or style) components, thus minimizing the impact of domain variation. In this work we combine feature disentanglement with graph convolutional networks (GCN) for unsupervised domain adaptation and apply it to two different standard medical imaging datasets for classification and compare it to SOTA methods.

Related Work: Prior works in UDA focused on medical image classification [2], object localisation, and lesion segmentation [29,39], and histopathology stain normalization [15]. Heimann et al. [29] used GANs to increase the size of training data and demonstrated improved localisation in X-ray fluoroscopy images. Likewise, Kamnitsas et al. [39] used GANs for improved lesion segmentation in magnetic resonance imaging (MRI). Ahn et al. [2] use a hierarchical unsupervised feature extractor to reduce reliance on annotated training data. Chang et al. [15] propose a novel stain mix-up for histopathology stain normalization and subsequent UDA for classification. Graph networks for UDA [52,178,99,5,98,4,100,101,97,96,118,105,23,3,123,32,161] have been used in medical imaging applications [1] such as brain surface segmentation [26] and brain image classification [30,31]. However, none of them combine feature disentanglement with GCNs for UDA.

Our Contributions: Although previous works used feature disentanglement and graph based domain adaptation separately, they did not combine them for medical image classification. In this work: 1) we propose a feature disentanglement module trained to align structural components coupled with a Graph

Convolutional Adversarial Network (GCAN) for unsupervised domain adaptation in medical images. 2) We perform feature disentanglement using swapped autoencoders to obtain texture and structural features, which are used for graph construction and defining generator losses. Since, in medical imaging applications, images from the same modality (showing the same organ) have similar texture, we introduce a novel cosine similarity loss components into the loss function that enforces the preservation of the structure component in the latent representation; 3) We demonstrate our method’s effectiveness on multiple medical image datasets.

2 Method

Given a source data set, $\mathcal{D}_S = \{(x_i^S, y_i^S)\}_{i=1}^{n_s}$, consisting of n_s labeled samples, and a target data set, $\mathcal{D}_T = \{(x_i^T)\}_{i=1}^{n_t}$ consisting of n_t unlabeled target samples, unsupervised domain adaptation aims to learn a classifier that can reliably classify unseen target samples. Here, $x_i^S \sim p_S$ is a source data point sampled from source distribution p_S , $y_i^S \in \mathcal{Y}_S$ is the label, and $x_i^T \sim p_T$ is a target data point sampled from target distribution p_T . As per the covariate shift assumption, we assume that $p_S(y|x) = p_T(y|x) \forall x$. Thus the only thing that changes between source and target is the distribution of the input samples, x .

The overall block diagram of our system is depicted in Figure 1. Our proposed approach consists of a feature disentanglement module (Figure 1-b) which separates semantic textural and structural features (often called style and content respectively). The output of the feature disentanglement module is constructed into a graph and then fed into an adversarial generator based graph neural network (Figure 1-a) that generates features which are domain invariant. The graph neural network learns more global relationships between samples, which in turn leads to more discriminative and domain invariant feature learning.

2.1 Feature Disentanglement Network:

Figure 1(b) shows the architecture of our feature disentanglement network (FDN). The FDN consists of two encoders ($E_S(\cdot), E_T(\cdot)$) and two decoder (generator) networks ($G_S(\cdot), G_T(\cdot)$), for the source and target domains respectively. Similar to a classic autoencoder, each encoder, $E_\bullet(\cdot)$, produces a latent code z_i for image $x_i^\bullet \sim p_\bullet$. Each decoder, $G_\bullet(\cdot)$, reconstructs the original image from z_i . Furthermore, we divide the latent code, z_i , into two components: a texture component, z_i^{tex} , and a structural component, z_i^{str} . Structural information is the local information that describes an image’s underlying structure and visible organs or parts, and is expected to be invariant across similar images from different domains. The disentanglement network is trained using the following loss function:

$$\mathcal{L}_{Disent} = \mathcal{L}_{Rec} + \lambda_1 \mathcal{L}_{swap} + \lambda_2 \mathcal{L}_{str} \quad (1)$$

\mathcal{L}_{Rec} , is the commonly used image reconstruction loss and is defined as:

$$\mathcal{L}_{Rec} = \mathbb{E}_{x_i^S \sim p_S} [\|x_i^S - G_S(E_S(x_i^S))\|] + \mathbb{E}_{x_j^T \sim p_T} [\|x_j^T - G_T(E_T(x_j^T))\|] \quad (2)$$

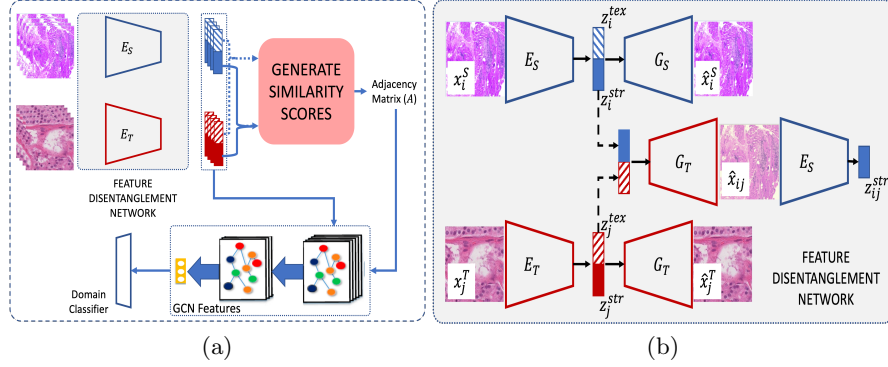


Fig. 1. (a) Workflow of our proposed method. Given images from source and target domains we disentangle features into texture and structure features, and generate similarity scores to construct an adjacency matrix. Generated features by the GCN are domain invariant and along with the latent features are used to train a domain classifier. (b) Architecture of feature disentanglement network with swapped structure features

As shown in Figure 1(b), we also combine the structure of source domain images (z_i^{str}) with the texture of target images (z_j^{tex}) and send it through G_T . The reconstructed images, \hat{x}_{ij} , should contain the structure of the original source domain image but, should look like an image from the target domain. To enforce this property, we use the adversarial loss term \mathcal{L}_{swap} defined as:

$$\mathcal{L}_{swap} = \mathbb{E}_{x_j \sim p_T} [\log(1 - D_{FD}(x_j))] + \mathbb{E}_{x_i \sim p^S, x_j \sim p^T} [\log(D_{FD}(G_T([z_i^{str}, z_j^{tex}])))]. \quad (3)$$

Here, D is a discriminator trained with target domain images, thus the generator should learn to produce images that appear to be from the target domain.

Furthermore, the newly generated image, \hat{x}_{ij} , should retain the structure of the original source domain image x_i^S from where the original structure was obtained. In [156] the authors use co-occurrent patch statistics from \hat{x}_{ij} and x_i^S such that any patch from x_i^S cannot be distinguished from a group of patches from \hat{x}_{ij} . This constraint is feasible in natural images since different images have far more varied style and content, but is challenging to implement in medical images since images from the same modality (showing the same organ) appear similar. Thus limited unique features are learnt under such a constraint. To overcome this limitation we introduce a novel component into the loss function. The output, \hat{x}_{ij} , when passed through encoder E_S produces the disintegrated features $z_{ij}^{str}, z_{ij}^{tex}$. Since \hat{x}_{ij} is generated from the combination of z_i^{str} and z_j^{tex} , z_{ij}^{str} should be similar to z_i^{str} (i.e. the structure should not change). This is enforced using the cosine similarity loss

$$\mathcal{L}_{str} = 1 - \langle z_i^{str}, z_{ij}^{str} \rangle \quad (4)$$

where $\langle \cdot \rangle$ denotes cosine similarity.

2.2 Graph Convolutional Adversarial Network

To learn more global relationships between samples, the features from the feature disentanglement module is used to construct an instance graph and which is processed with a Graph Convolutional Network (GCN). The GCN learns layer-wise propagation operations that can be applied directly on graphs. Given an undirected graph with m nodes, the set of edges between nodes, and an adjacency matrix $\mathbf{A} \in R^{m \times m}$, a linear transformation of graph convolution is defined as the multiplication of a graph signal $\mathbf{X} \in R^{k \times m}$ with a filter $\mathbf{W} \in R^{k \times c}$:

$$\mathbf{Z} = \hat{\mathbf{D}}^{-\frac{1}{2}} \hat{\mathbf{A}} \hat{\mathbf{D}}^{-\frac{1}{2}} \mathbf{X}^T \mathbf{W}, \quad (5)$$

where $\hat{\mathbf{A}} = \mathbf{A} + \mathbf{I}$, \mathbf{I} being the identity matrix, and $\hat{\mathbf{D}}_{ii} = \sum_j \hat{\mathbf{A}}_{ij}$. The output is a $c \times m$ matrix \mathbf{Z} . The GCN can be constructed by stacking multiple graph convolutional layers followed by a non-linear operation (such as ReLU).

In our implementation, each node in the instance graph represents a latent feature of a sample (either source or target domain) $[z^{tex}, z^{str}]$. The adjacency matrix is constructed using the cosine similarity score as $\hat{\mathbf{A}} = \mathbf{X}_{sc} \mathbf{X}_{sc}^T$. Note that the cosine similarity score quantifies the semantic similarity between two samples. Here $\mathbf{X}_{sc} \in R^{w \times h}$ is the matrix of cosine similarity scores, w is the batch size, and $h = 2$ is the dimension of the similarity scores of each sample obtained from corresponding $[z^{tex}, z^{str}]$.

The flow of our proposed approach is shown in Figure 1(a). Our network is trained by minimizing the following objective function:

$$\mathcal{L}(\mathcal{X}_S, \mathcal{Y}_S, \mathcal{X}_T) = \mathcal{L}_C(\mathcal{X}_S, \mathcal{Y}_S) + \lambda_{adv} \mathcal{L}_{Adv}(\mathcal{X}_S, \mathcal{X}_T) \quad (6)$$

The classification loss \mathcal{L}_C is a cross entropy loss $\mathcal{L}_C(\mathcal{X}_S, \mathcal{Y}_S) = -\sum_{c=1}^{n_s} y_c \log(p_c)$, y_c is the indicator variable and p_c is the class probability.

The second loss component is an adversarial loss function defined in Eq. 7. A domain classifier D identifies whether features from the graph neural network G_{GNN} are from the source or target domain. Conversely, G_{GNN} , is being trained to produce samples that can fool D . This two-player minimax game will reach an equilibrium state when features from G_{GNN} are domain-invariant.

$$\mathcal{L}_{Adv}(\mathcal{X}_S, \mathcal{X}_T) = \mathbb{E}_{x \in D_S} [\log(1 - D(G_{GNN}(x)))] + \mathbb{E}_{x \in D_T} [\log(D(G_{GNN}(x)))] \quad (7)$$

Training And Implementation: Given \mathbf{X} and \mathbf{A} the GCN features are obtained according to Eq.5. Source and target domain graphs are individually constructed and fed into the parameters-shared GCNs to learn representations. The dimension of z^{tex} is 256, while z^{str} is 64×64 . **VAE Network:** The encoder consists of 3 convolution blocks followed by max pooling. The decoder is symmetrically designed to the encoder. 3×3 convolution filters are used and 64, 32, 32 filters are used in each conv layer. The input to the VAE is 256×256 . For the domain classifier we use DenseNet-121 network with pre-trained weights from ImageNet and fine-tuned using self supervised learning. As a pre-text task we use the classifier to predict the intensity values of masked regions.

3 Experiments And Results

3.1 Results For CAMELYON17 Dataset

Dataset Description: We use the CAMELYON17 dataset [14] to evaluate the performance of the proposed method on tumor/normal classification. In this dataset, a total of 500 *H&E* stained WSIs are collected from five medical centers (denoted as by $C_{117}, C_{217}, C_{317}, C_{417}, C_{517}$ respectively). 50 of these WSIs include lesion-level annotations. All positive and negative WSIs are randomly split into training/validation/test sets and provided by the organizers in a 50/30/20% split for the individual medical centers to obtain the following split: C_{117} :37/22/15, C_{217} : 34/20/14, C_{317} : 43/24/18, C_{417} : 35/20/15, C_{517} : 36/20/15. 256×256 image patches are extracted from the annotated tumors for positive patches and from tissue regions of WSIs without tumors for negative patches. We use $\lambda_1 = 0.9, \lambda_2 = 1.2, \lambda_{adv} = 1.3$.

Implementation Details Since the images have been taken from different medical centers their appearance varies despite sharing the same disease labels. This is due to slightly different protocols of *H&E* staining. Stain normalization has been a widely explored topic which aims to standardize the appearance of images across all centers, which is equivalent to domain adaptation. Recent approaches to stain normalization/domain adaptation favour use of GANs and other deep learning methods. We compare our approach to recent approaches and also with [15] which explicitly performs UDA using MixUp.

To evaluate our method’s performance: 1) We use C_{117} as the source dataset and train a ResNet-50 classifier [28] (ResNet $_{C1}$). Each remaining dataset from the other centers are, separately, taken as the target dataset, the corresponding domain adapted images are generated, and classified using ResNet $_{C1}$. As a baseline, we perform the experiment without domain adaptation denoted as *No – UDA* where ResNet $_{C1}$ is used to classify images from other centers. We report results for a network trained in a fully-supervised manner on the training set from the same domain (*FSL – SameDomain*) to give an upper-bound expectation for a UDA model trained on other domain’s data, where a ResNet-50 is trained on the training images and used to classify test images, all from the same hospital. This approach will give the best results for a given classifier (in our case ResNet-50). All the above experiments are repeated using each of $C_{217}, C_{317}, C_{417}, C_{517}$ as the source dataset. Table 1 summarizes our results. PyTorch was used in all implementations.

The results in Table 1 show that UDA methods are better than conventional stain normalization approaches as evidenced by the superior performance of our proposed method and [15]. Our method performs the best amongst all the methods, and approaches *FSL – SameDomain*, the theoretical maximum performance a domain adaptation method can achieve. This shows that our proposed GCN based approach performs better than other UDA methods. The ablation studies also show that our proposed individual loss term \mathcal{L}_{Str} has a significant contribution to the overall performance of our method and excluding it significantly degrades the performance.

	Comparison and Proposed Method							Proposed Method	Ablation Study Results		
	No UDA	MMD	CycleGAN	[174]	[21]	[84]	[15]		FSL-Same	\mathcal{L}_{Str}	\mathcal{L}_{Swap}
<i>Center 1</i>	0.8068	0.8742	0.9010	0.9123	0.9487	0.9668	0.979	0.988	0.991	0.979	0.953
<i>Center 2</i>	0.7203	0.6926	0.7173	0.7347	0.8115	0.8537	0.948	0.963	0.972	0.951	0.941
<i>Center 3</i>	0.7027	0.8711	0.8914	0.9063	0.8727	0.9385	0.946	0.958	0.965	0.948	0.932
<i>Center 4</i>	0.8289	0.8578	0.8811	0.8949	0.9235	0.9548	0.965	0.979	0.986	0.967	0.949
<i>Center 5</i>	0.8203	0.7854	0.8102	0.8223	0.9351	0.9462	0.942	0.949	0.957	0.934	0.921
<i>Average</i>	0.7758	0.8162	0.8402	0.8541	0.8983	0.9320	0.956	0.967	0.974	0.956	0.939
<i>p</i>	0.0001	0.0001	0.002	0.003	0.013	0.024	0.017	-	0.07	0.01	0.001

Table 1. Classification results in terms of AUC measures for different domain adaptation methods on the CAMELYON17 dataset. Note: *FSL – SD* is a fully-supervised model trained on target domain data.

3.2 Results on Chest Xray Dataset

We use the following chest Xray datasets: **NIH Chest Xray Dataset:** The NIH ChestXray14 dataset [177] has 112,120 expert-annotated frontal-view X-rays from 30,805 unique patients and has 14 disease labels. Original images were resized to 256×256 , and $\lambda_1 = 0.9, \lambda_2 = 1.2, \lambda_{adv} = 1.2$. **CheXpert Dataset:** This dataset [33] has 224,316 chest radiographs of 65,240 patients labeled for the presence of 14 common chest conditions. The validation ground-truth is obtained using majority voting from annotations of 3 board-certified radiologists. Original images were resized to 256×256 , and $\lambda_1 = 0.95, \lambda_2 = 1.1, \lambda_{adv} = 1.3$. These two datasets have the same set of disease labels.

We divide both datasets into train/validation/test splits on the patient level at 70/10/20 ratio, such that images from one patient are in only one of the splits. Then we train a DenseNet-121 [158] classifier on one dataset (say NIH’s train split). Here the NIH dataset serves as the source data and CheXpert is the target dataset. We then apply the trained model on the training split of the NIH dataset and tested on the test split of the same domain the results are denoted as *FSL – Same*. When we apply this model to the test split of the CheXpert data without domain adaptation the results are reported under *No-UDA*.

Tables 2,3 show classification results for different DA techniques where, respectively, the NIH and CheXpert dataset were the source domain and the performance metrics are for, respectively, CheXpert and NIH dataset’s *test split*. We observe that UDA methods perform worse than *FSL – Same*. This is expected since it is very challenging to perfectly account for domain shift. However all UDA methods perform better than fully supervised methods trained on one domain and applied on another without domain adaptation.

The DANN architecture [22] outperforms MMD and cycleGANs, and is on par with graph convolutional methods GCAN [52] and GCN2 [31]. However our method outperforms all compared methods which can be attributed to the combination of GCNs, which learn more useful global relationships between different samples, and feature disentanglement which in turn leads to more discriminative feature learning.

	Atel.	Card.	Eff.	Infil.	Mass	Nodule	Pneu.	Pneumot.	Consol.	Edema	Emphy.	Fibr.	PT.	Hernia
No UDA	0.697	0.814	0.761	0.652	0.739	0.694	0.703	0.781	0.704	0.792	0.815	0.719	0.728	0.811
MMD	0.741	0.851	0.801	0.699	0.785	0.738	0.748	0.807	0.724	0.816	0.831	0.745	0.754	0.846
CycleGANs	0.765	0.874	0.824	0.736	0.817	0.758	0.769	0.832	0.742	0.838	0.865	0.762	0.773	0.864
DANN	0.792	0.902	0.851	0.761	0.849	0.791	0.802	0.869	0.783	0.862	0.894	0.797	0.804	0.892
FSL-Same	0.849	0.954	0.903	0.814	0.907	0.825	0.844	0.928	0.835	0.928	0.951	0.847	0.842	0.941
GCAN	0.798	0.908	0.862	0.757	0.858	0.803	0.800	0.867	0.776	0.865	0.908	0.811	0.799	0.904
GCN2	0.809	0.919	0.870	0.765	0.871	0.807	0.810	0.882	0.792	0.883	0.921	0.817	0.812	0.914
Proposed	0.825	0.931	0.884	0.788	0.890	0.818	0.828	0.903	0.818	0.910	0.934	0.828	0.830	0.923
Ablation Study Results														
\mathcal{L}_{Str}	0.811	0.914	0.870	0.771	0.872	0.808	0.819	0.884	0.803	0.887	0.916	0.809	0.812	0.907
\mathcal{L}_{Swap}	0.787	0.885	0.845	0.741	0.843	0.780	0.791	0.856	0.776	0.859	0.887	0.785	0.786	0.883

Table 2. Classification results on the CheXpert dataset’s test split using NIH data as the source domain. Note: *FSL – SD* is a fully-supervised model trained on target domain data.

	Atel.	Card.	Eff.	Infil.	Mass	Nodule	Pneu.	Pneumot.	Consol.	Edema	Emphy.	Fibr.	PT	Hernia
No UDA	0.718	0.823	0.744	0.730	0.739	0.694	0.683	0.771	0.712	0.783	0.803	0.711	0.710	0.785
MMD	0.734	0.846	0.762	0.741	0.785	0.738	0.709	0.793	0.731	0.801	0.821	0.726	0.721	0.816
CycleGANs	0.751	0.861	0.785	0.761	0.817	0.758	0.726	0.814	0.746	0.818	0.837	0.741	0.737	0.836
DANN	0.773	0.882	0.819	0.785	0.837	0.791	0.759	0.838	0.770	0.836	0.863	0.766	0.762	0.861
FSL-Same	0.814	0.929	0.863	0.821	0.869	0.825	0.798	0.863	0.805	0.872	0.904	0.802	0.798	0.892
GCAN	0.78	0.895	0.811	0.777	0.828	0.782	0.751	0.832	0.765	0.828	0.857	0.761	0.756	0.851
GCN2	0.786	0.906	0.833	0.789	0.831	0.802	0.763	0.835	0.774	0.837	0.868	0.768	0.763	0.860
Proposed	0.798	0.931	0.884	0.799	0.843	0.818	0.773	0.847	0.784	0.849	0.879	0.779	0.774	0.868
Ablation Study Results														
\mathcal{L}_{Str}	0.788	0.919	0.875	0.786	0.832	0.804	0.768	0.834	0.778	0.835	0.863	0.766	0.765	0.853
\mathcal{L}_{Swap}	0.770	0.903	0.860	0.771	0.811	0.788	0.748	0.814	0.761	0.816	0.845	0.746	0.749	0.836

Table 3. Classification results on the NIH Xray dataset’s test split using CheXpert data as the source domain. Note: *FSL – SD* is a fully-supervised model trained on target domain data.

4 Conclusion

In this paper we propose an UDA method using graph adversarial convolutional networks and feature disentanglement using a novel loss term. Our novel loss term extends the swapped autoencoder architecture thus learning more discriminative features. Our graph convolutional network based unsupervised domain adaptation method outperforms conventional CNN methods as graphs better learn the interaction between samples by focusing on more global interactions while CNNs focus on the local neighborhood. This enables GCN to perform better UDA as demonstrated by results on multiple datasets. While feature disentanglement also contributes to improved performance, there is scope for improvement. In future work we wish to explore stronger disentanglement techniques, and aim to extend this approach for segmentation-based tasks.

References

1. Ahmedt-Aristizabal, D., Armin, M.A., Denman, S., Fookes, C., Petersson, L.: Graph-based deep learning for medical diagnosis and analysis: Past, present and

- future. *Sensors* **21**(14), 47–58 (Jul 2021)
2. Ahn, E., Kumar, A., Fulham, M., Feng, D., Kim, J.: Unsupervised domain adaptation to classify medical images using zero-bias convolutional auto-encoders and context-based feature augmentation. *IEEE TMI* **39**(7), 2385–2394 (2020)
 3. Antony, B., Sedai, S., Mahapatra, D., Garnavi, R.: Real-time passive monitoring and assessment of pediatric eye health. In: US Patent App. 16/178,757 (2020)
 4. Bastide, P., Kiral-Kornek, I., Mahapatra, D., Saha, S., Vishwanath, A., Cavallar, S.V.: Machine learned optimizing of health activity for participants during meeting times. In: US Patent App. 15/426,634 (2018)
 5. Bastide, P., Kiral-Kornek, I., Mahapatra, D., Saha, S., Vishwanath, A., Cavallar, S.V.: Visual health maintenance and improvement. In: US Patent 9,993,385 (2018)
 6. Bastide, P., Kiral-Kornek, I., Mahapatra, D., Saha, S., Vishwanath, A., Cavallar, S.V.: Crowdsourcing health improvements routes. In: US Patent App. 15/611,519 (2019)
 7. Bozorgtabar, B., Mahapatra, D., von Teng, H., Pollinger, A., Ebner, L., Thiran, J.P., Reyes, M.: Informative sample generation using class aware generative adversarial networks for classification of chest xrays. *Computer Vision and Image Understanding* **184**, 57–65 (2019)
 8. Bozorgtabar, B., Mahapatra, D., von Teng, H., Pollinger, A., Ebner, L., Thiran, J.P., Reyes, M.: Informative sample generation using class aware generative adversarial networks for classification of chest xrays. In: arXiv preprint arXiv:1904.10781 (2019)
 9. Bozorgtabar, B., Mahapatra, D., Thiran, J.P.: Exprada: Adversarial domain adaptation for facial expression analysis. In *Press Pattern Recognition* **100**, 15–28 (2020)
 10. Bozorgtabar, B., Mahapatra, D., Thiran, J.P., Shao, L.: SALAD: Self-supervised aggregation learning for anomaly detection on x-rays. In: *In Proc. MICCAI*. pp. 468–478 (2020)
 11. Bozorgtabar, B., Mahapatra, D., Vray, G., Thiran, J.P.: Anomaly detection on x-rays using self-supervised aggregation learning. In: arXiv preprint arXiv:2010.09856 (2020)
 12. Bozorgtabar, B., Mahapatra, D., Zlobec, I., Rau, T., Thiran, J.: Computational pathology. *Frontiers in Medicine* **7** (2020)
 13. Bozorgtabar, B., Rad, M.S., Mahapatra, D., Thiran, J.P.: Syndemo: Synergistic deep feature alignment for joint learning of depth and ego-motion. In: *In Proc. IEEE ICCV* (2019)
 14. Bándi, P., , et al.: From Detection of Individual Metastases to Classification of Lymph Node Status at the Patient Level: The CAMELYON17 Challenge. *IEEE Trans. Med. Imag.* **38**(2), 550–560 (2019)
 15. Chang, J.R., Wu, M.S., et al.: Stain mix-up: Unsupervised domain generalization for histopathology images. In: *MICCAI 2021*. pp. 117–126 (2021)
 16. Chen, C., Dou, Q., Chen, H., et al.: Unsupervised bidirectional cross-modality adaptation via deeply synergistic image and feature alignment for medical image segmentation. *IEEE Trans. Med. Imag.* **39**(7), 2494–2505 (2020)
 17. Das, S.D., Dutta, S., Shah, N.A., Mahapatra, D., Ge, Z.: Anomaly detection in retinal images using multi-scale deep feature sparse coding. In: *2022 IEEE 19th International Symposium on Biomedical Imaging (ISBI)*. pp. 1–5 (2022). <https://doi.org/10.1109/ISBI52829.2022.9761713>
 18. Das, S.D., Dutta, S., Shah, N.A., Mahapatra, D., Ge, Z.: Anomaly detection in retinal images using multi-scale deep feature sparse coding. In: arXiv preprint arXiv:2201.11506 (2022)

19. Devika, K., Mahapatra, D., Subramanian, R., Oruganti, V.R.M.: Outlier-based autism detection using longitudinal structural mri. *IEEE Access* **10**, 27794–27808 (2022). <https://doi.org/10.1109/ACCESS.2022.3157613>
20. Devika, K., Mahapatra, D., Subramanian, R., Oruganti, V.R.M.: Outlier-based autism detection using longitudinal structural mri. In: arXiv preprint arXiv:2202.09988 (2022)
21. Gadermayr, M., Appel, V., et al.: Which way round?: A study on the performance of stain-translation for segmenting arbitrarily dyed histological images. In: *MICCAI (I)*. pp. 165–173 (2018)
22. Ganin, Y., Ustinova, E., et al.: Domain-adversarial training of neural networks (2016)
23. Garnavi, R., Mahapatra, D., Roy, P., Tennakoon, R.: System and method to teach and evaluate image grading performance using prior learned expert knowledge base. In: *US Patent App.* 10,657,838 (2020)
24. Ge, Z., Mahapatra, D., Chang, X., Chen, Z., Chi, L., Lu, H.: Improving multi-label chest x-ray disease diagnosis by exploiting disease and health labels dependencies. In *press Multimedia Tools and Application* pp. 1–14 (2019)
25. Ge, Z., Mahapatra, D., Sedai, S., Garnavi, R., Chakravorty, R.: Chest x-rays classification: A multi-label and fine-grained problem. In: arXiv preprint arXiv:1807.07247 (2018)
26. Gopinath, K., Desrosiers, C., Lombaert, H.: Graph domain adaptation for alignment-invariant brain surface segmentation (2020)
27. Gulshan, V., Peng, L., , et. al.: Development and Validation of a Deep Learning Algorithm for Detection of Diabetic Retinopathy in Retinal Fundus Photographs. *JAMA* **316**(22), 2402–2410 (12 2016)
28. He, K., Zhang, X., Ren, S., Sun, J.: Deep residual learning for image recognition. In: *In Proc. CVPR* (2016)
29. Heimann, T., Mountney, P., John, M., Ionasec, R.: Learning without labeling: Domain adaptation for ultrasound transducer localization. In: *MICCAI 2013*. pp. 49–56 (2013)
30. Hong, Y., Chen, G., Yap, P.T., Shen, D.: Multifold acceleration of diffusion mri via deep learning reconstruction from slice-undersampled data. In: *IPMI*. pp. 530–541 (2019)
31. Hong, Y., Kim, J., Chen, G., Lin, W., Yap, P.T., Shen, D.: Longitudinal prediction of infant diffusion mri data via graph convolutional adversarial networks. *IEEE Transactions on Medical Imaging* **38**(12), 2717–2725 (2019)
32. Hoog, J.D., Mahapatra, D., Garnavi, R., Jalali, F.: Personalized monitoring of injury rehabilitation through mobile device imaging. In: *US Patent App.* 16/589,046 (2021)
33. Irvin, J., Rajpurkar, P., et. al.: CheXpert: A large chest radiograph dataset with uncertainty labels and expert comparison. In: arXiv preprint arXiv:1901.07031 (2017)
34. Ju, L., Wang, X., Wang, L., Liu, T., Zhao, X., Drummond, T., Mahapatra, D., Ge, Z.: Relational subsets knowledge distillation for long-tailed retinal diseases recognition. In: arXiv preprint arXiv:2104.11057 (2021)
35. Ju, L., Wang, X., Wang, L., Mahapatra, D., Zhao, X., Harandi, M., Drummond, T., Liu, T., Ge, Z.: Improving medical image classification with label noise using dual-uncertainty estimation. In: arXiv preprint arXiv:2103.00528 (2020)
36. Ju, L., Wang, X., Wang, L., Mahapatra, D., Zhao, X., Zhou, Q., Liu, T., Ge, Z.: Improving medical images classification with label noise using dual-

- uncertainty estimation. *IEEE Transactions on Medical Imaging* pp. 1–1 (2022). <https://doi.org/10.1109/TMI.2022.3141425>
37. Ju, L., Wang, X., Zhao, X., Lu, H., Mahapatra, D., Bonnington, P., Ge, Z.: Synergic adversarial label learning for grading retinal diseases via knowledge distillation and multi-task learning. *IEEE JBHI* **100**, 1–14 (2020)
 38. Ju, L., Wang, X., Zhao, X., Lu, H., Mahapatra, D., Ge, Z.: Relational subsets knowledge distillation for long-tailed retinal diseases recognition. In: *MICCAI 2021*. pp. 1–11 (2021)
 39. Kamnitsas, K., Baumgartner, C., et al.: Unsupervised domain adaptation in brain lesion segmentation with adversarial networks. In: *IPMI*. pp. 597–609 (2017)
 40. Kuanar, S., Athitsos, V., Mahapatra, D., Rajan, A.: Multi-scale deep learning architecture for nucleus detection in renal cell carcinoma microscopy image. In: *arXiv preprint arXiv:2104.13557* (2021)
 41. Kuanar, S., Athitsos, V., Mahapatra, D., Rao, K., Akhtar, Z., Dasgupta, D.: Low dose abdominal ct image reconstruction: An unsupervised learning based approach. In: *Proc. IEEE ICIP*. pp. 1351–1355 (2019)
 42. Kuanar, S., Mahapatra, D., Athitsos, V., Rao, K.: Gated fusion network for sao filter and inter frame prediction in versatile video coding. In: *arXiv preprint arXiv:2105.12229* (2021)
 43. Kuanar, S., Rao, K., Mahapatra, D., Bilas, M.: Night time haze and glow removal using deep dilated convolutional network. In: *arXiv preprint arXiv:1902.00855* (2019)
 44. Kuanar, S., Mahapatra, D., Bilas, M., Rao, K.: Multi-path dilated convolution network for haze and glow removal in night time images. *The Visual Computer* **38**(3), 1121–1134 (2022)
 45. Kuang, H., Guthier, B., Saini, M., Mahapatra, D., Saddik, A.E.: A real-time smart assistant for video surveillance through handheld devices. In: *Proc. ACM Intl. Conf. Multimedia*. pp. 917–920 (2014)
 46. Kumagai, A., Iwata, T.: Unsupervised domain adaptation by matching distributions based on the maximum mean discrepancy via unilateral transformations **33**, 4106–4113 (Jul 2019)
 47. Li, F., Li, W., Qin, S., Wang, L.: Mdfa-net: Multiscale dual-path feature aggregation network for cardiac segmentation on multi-sequence cardiac mr. *Knowledge-Based Systems* **215**, 106776 (2021)
 48. Li, Z., Mahapatra, D., J.Tielbeek, Stoker, J., van Vliet, L., Vos, F.: Image registration based on autocorrelation of local structure. *IEEE Trans. Med. Imaging* **35**(1), 63–75 (2016)
 49. Liu, A.H., Liu, Y.C., Yeh, Y.Y., Wang, Y.C.F.: A unified feature disentangler for multi-domain image translation and manipulation. *Advances in neural information processing systems* **31** (2018)
 50. Liu, Y., Gadepalli, K., et al.: Detecting cancer metastases on gigapixel pathology images. In: *arXiv preprint arXiv:1703.02442* (2017)
 51. Luo, Z., Zou, Y., et al.: Label efficient learning of transferable representations across domains and tasks. In: *Proceedings of NeurIPS*. p. 164–176 (2017)
 52. Ma, X., Zhang, T., Xu, C.: Gcan: Graph convolutional adversarial network for unsupervised domain adaptation. In: *IEEE CVPR*. pp. 8258–8268 (2019)
 53. Mahapatra, D.: Elastic registration of cardiac perfusion images using saliency information. *Sequence and Genome Analysis – Methods and Applications* pp. 351–364 (2011)

54. Mahapatra, D.: Neonatal brain mri skull stripping using graph cuts and shape priors. In: In Proc: MICCAI workshop on Image Analysis of Human Brain Development (IAHBD) (2011)
55. Mahapatra, D.: Cardiac lv and rv segmentation using mutual context information. In: Proc. MICCAI-MLMI. pp. 201–209 (2012)
56. Mahapatra, D.: Groupwise registration of dynamic cardiac perfusion images using temporal information and segmentation information. In: In Proc: SPIE Medical Imaging (2012)
57. Mahapatra, D.: Landmark detection in cardiac mri using learned local image statistics. In: Proc. MICCAI-Statistical Atlases and Computational Models of the Heart. Imaging and Modelling Challenges (STACOM). pp. 115–124 (2012)
58. Mahapatra, D.: Skull stripping of neonatal brain mri: Using prior shape information with graphcuts. *J. Digit. Imaging* **25**(6), 802–814 (2012)
59. Mahapatra, D.: Cardiac image segmentation from cine cardiac mri using graph cuts and shape priors. *J. Digit. Imaging* **26**(4), 721–730 (2013)
60. Mahapatra, D.: Cardiac mri segmentation using mutual context information from left and right ventricle. *J. Digit. Imaging* **26**(5), 898–908 (2013)
61. Mahapatra, D.: Graph cut based automatic prostate segmentation using learned semantic information. In: Proc. IEEE ISBI. pp. 1304–1307 (2013)
62. Mahapatra, D.: Joint segmentation and groupwise registration of cardiac perfusion images using temporal information. *J. Digit. Imaging* **26**(2), 173–182 (2013)
63. Mahapatra, D.: An automated approach to cardiac rv segmentation from mri using learned semantic information and graph cuts. *J. Digit. Imaging*. **27**(6), 794–804 (2014)
64. Mahapatra, D.: Combining multiple expert annotations using semi-supervised learning and graph cuts for medical image segmentation. *Computer Vision and Image Understanding* **151**(1), 114–123 (2016)
65. Mahapatra, D.: Retinal image quality classification using neurobiological models of the human visual system. In: In Proc. MICCAI-OMIA. pp. 1–8 (2016)
66. Mahapatra, D.: Consensus based medical image segmentation using semi-supervised learning and graph cuts. In: arXiv preprint arXiv:1612.02166 (2017)
67. Mahapatra, D.: Semi-supervised learning and graph cuts for consensus based medical image segmentation. *Pattern Recognition* **63**(1), 700–709 (2017)
68. Mahapatra, D.: Amd severity prediction and explainability using image registration and deep embedded clustering. In: arXiv preprint arXiv:1907.03075 (2019)
69. Mahapatra, D.: Generative adversarial networks and domain adaptation for training data independent image registration. In: arXiv preprint arXiv:1910.08593 (2019)
70. Mahapatra, D.: Registration of histopathology images using structural information from fine grained feature maps. In: arXiv preprint arXiv:2007.02078 (2020)
71. Mahapatra, D.: Interpretability-driven sample selection using self supervised learning for disease classification and segmentation. In: arXiv preprint arXiv:2104.06087 (2021)
72. Mahapatra, D.: Learning of inter-label geometric relationships using self-supervised learning: Application to gleason grade segmentation. In: arXiv preprint arXiv:2110.00404 (2021)
73. Mahapatra, D., Agarwal, K., Khosrowabadi, R., Prasad, D.: Recent advances in statistical data and signal analysis: Application to real world diagnostics from medical and biological signals. In: *Computational and mathematical methods in medicine* (2016)

74. Mahapatra, D., Antony, B., Sedai, S., Garnavi, R.: Deformable medical image registration using generative adversarial networks. In: In Proc. IEEE ISBI. pp. 1449–1453 (2018)
75. Mahapatra, D., Bozorgtabar, B.: Retinal vasculature segmentation using local saliency maps and generative adversarial networks for image super resolution. In: arXiv preprint arXiv:1710.04783 (2017)
76. Mahapatra, D., Bozorgtabar, B.: Progressive generative adversarial networks for medical image super resolution. In: arXiv preprint arXiv:1902.02144 (2019)
77. Mahapatra, D., Bozorgtabar, B., Garnavi, R.: Image super-resolution using progressive generative adversarial networks for medical image analysis. *Computerized Medical Imaging and Graphics* **71**, 30–39 (2019)
78. Mahapatra, D., Bozorgtabar, B., Ge, Z.: Medical image classification using generalized zero shot learning. In: In IEEE CVAMD 2021. pp. 3344–3353 (2021)
79. Mahapatra, D., Bozorgtabar, B., Kuanar, S., Ge, Z.: Self-supervised multimodal generalized zero shot learning for gleason grading. In: In MICCAI-DART 2021. pp. 1–11 (2021)
80. Mahapatra, D., Bozorgtabar, B., Shao, L.: Pathological retinal region segmentation from oct images using geometric relation based augmentation. In: In Proc. IEEE CVPR. pp. 9611–9620 (2020)
81. Mahapatra, D., Bozorgtabar, B., Thiran, J.P., Shao, L.: Pathological retinal region segmentation from oct images using geometric relation based augmentation. In: arXiv preprint arXiv:2003.14119 (2020)
82. Mahapatra, D., Bozorgtabar, B., Thiran, J.P., Shao, L.: Structure preserving stain normalization of histopathology images using self supervised semantic guidance. In: In Proc. MICCAI. pp. 309–319 (2020)
83. Mahapatra, D., Bozorgtabar, B., Thiran, J.P., Shao, L.: Structure preserving stain normalization of histopathology images using self supervised semantic guidance. In: arXiv preprint arXiv:2008.02101 (2020)
84. Mahapatra, D., Bozorgtabar, B., Thiran, J.P., Shao, L.: Structure preserving stain normalization of histopathology images using self supervised semantic guidance. In: In Proc. MICCAI. pp. 309–319 (2020)
85. Mahapatra, D., Bozorgtabar, S., Hewavitharanage, S., Garnavi, R.: Image super resolution using generative adversarial networks and local saliency maps for retinal image analysis. In: In Proc. MICCAI. pp. 382–390 (2017)
86. Mahapatra, D., Bozorgtabar, S., Thiran, J.P., Reyes, M.: Efficient active learning for image classification and segmentation using a sample selection and conditional generative adversarial network. In: In Proc. MICCAI (2). pp. 580–588 (2018)
87. Mahapatra, D., Buhmann, J.: Obtaining consensus annotations for retinal image segmentation using random forest and graph cuts. In: In Proc. OMIA. pp. 41–48 (2015)
88. Mahapatra, D., Buhmann, J.: Visual saliency based active learning for prostate mri segmentation. In: In Proc. MLMI. pp. 9–16 (2015)
89. Mahapatra, D., Buhmann, J.: Visual saliency-based active learning for prostate magnetic resonance imaging segmentation. *SPIE Journal of Medical Imaging* **3**(1), 014003 (2016)
90. Mahapatra, D., Buhmann, J.: Automatic cardiac rv segmentation using semantic information with graph cuts. In: Proc. IEEE ISBI. pp. 1094–1097 (2013)
91. Mahapatra, D., Buhmann, J.: Analyzing training information from random forests for improved image segmentation. *IEEE Trans. Imag. Proc.* **23**(4), 1504–1512 (2014)

92. Mahapatra, D., Buhmann, J.: Prostate mri segmentation using learned semantic knowledge and graph cuts. *IEEE Trans. Biomed. Engg.* **61**(3), 756–764 (2014)
93. Mahapatra, D., Buhmann, J.: A field of experts model for optic cup and disc segmentation from retinal fundus images. In: *In Proc. IEEE ISBI*. pp. 218–221 (2015)
94. Mahapatra, D., Garnavi, R., Roy, P., Tennakoon, R.: System and method to teach and evaluate image grading performance using prior learned expert knowledge base. In: *US Patent App. 15/459,457* (2018)
95. Mahapatra, D., Garnavi, R., Roy, P., Tennakoon, R.: System and method to teach and evaluate image grading performance using prior learned expert knowledge base. In: *US Patent App. 15/814,590* (2018)
96. Mahapatra, D., Garnavi, R., Sedai, S., Roy, P.: Joint segmentation and characteristics estimation in medical images. In: *US Patent App. 15/234,426* (2017)
97. Mahapatra, D., Garnavi, R., Sedai, S., Roy, P.: Retinal image quality assessment, error identification and automatic quality correction. In: *US Patent 9,779,492* (2017)
98. Mahapatra, D., Garnavi, R., Sedai, S., Tennakoon, R.: Classification of severity of pathological condition using hybrid image representation. In: *US Patent App. 15/426,634* (2018)
99. Mahapatra, D., Garnavi, R., Sedai, S., Tennakoon, R.: Generating an enriched knowledge base from annotated images. In: *US Patent App. 15/429,735* (2018)
100. Mahapatra, D., Garnavi, R., Sedai, S., Tennakoon, R., Chakravorty, R.: Early prediction of age related macular degeneration by image reconstruction. In: *US Patent App. 15/854,984* (2018)
101. Mahapatra, D., Garnavi, R., Sedai, S., Tennakoon, R., Chakravorty, R.: Early prediction of age related macular degeneration by image reconstruction. In: *US Patent 9,943,225* (2018)
102. Mahapatra, D., Ge, Z.: Combining transfer learning and segmentation information with gans for training data independent image registration. In: *arXiv preprint arXiv:1903.10139* (2019)
103. Mahapatra, D., Ge, Z.: Training data independent image registration with gans using transfer learning and segmentation information. In: *In Proc. IEEE ISBI*. pp. 709–713 (2019)
104. Mahapatra, D., Ge, Z.: Training data independent image registration using generative adversarial networks and domain adaptation. *Pattern Recognition* **100**, 1–14 (2020)
105. Mahapatra, D., Ge, Z., Sedai, S.: Joint registration and segmentation of images using deep learning. In: *US Patent App. 16/001,566* (2019)
106. Mahapatra, D., Ge, Z., Sedai, S., Chakravorty, R.: Joint registration and segmentation of xray images using generative adversarial networks. In: *In Proc. MICCAI-MLMI*. pp. 73–80 (2018)
107. Mahapatra, D., Gilani, S., Saini, M.: Coherency based spatio-temporal saliency detection for video object segmentation. *IEEE Journal of Selected Topics in Signal Processing*. **8**(3), 454–462 (2014)
108. Mahapatra, D., J.Tielbeek, Makanyanga, J., Stoker, J., Taylor, S., Vos, F., Buhmann, J.: Automatic detection and segmentation of crohn’s disease tissues from abdominal mri. *IEEE Trans. Med. Imaging* **32**(12), 1232–1248 (2013)
109. Mahapatra, D., J.Tielbeek, Makanyanga, J., Stoker, J., Taylor, S., Vos, F., Buhmann, J.: Active learning based segmentation of crohn’s disease using principles of visual saliency. In: *Proc. IEEE ISBI*. pp. 226–229 (2014)

110. Mahapatra, D., J.Tielbeek, Makanyanga, J., Stoker, J., Taylor, S., Vos, F., Buhmann, J.: Combining multiple expert annotations using semi-supervised learning and graph cuts for crohn's disease segmentation. In: In Proc: MICCAI-ABD (2014)
111. Mahapatra, D., J.Tielbeek, Vos, F., Buhmann, J.: A supervised learning approach for crohn's disease detection using higher order image statistics and a novel shape asymmetry measure. *J. Digit. Imaging* **26**(5), 920–931 (2013)
112. Mahapatra, D., Kuanar, S., Bozorgtabar, B., Ge, Z.: Self-supervised learning of inter-label geometric relationships for gleason grade segmentation. In: In MICCAI-DART 2021. pp. 57–67 (2021)
113. Mahapatra, D., Li, Z., Vos, F., Buhmann, J.: Joint segmentation and groupwise registration of cardiac dce mri using sparse data representations. In: In Proc. IEEE ISBI. pp. 1312–1315 (2015)
114. Mahapatra, D., Routray, A., Mishra, C.: An active snake model for classification of extreme emotions. In: IEEE International Conference on Industrial Technology (ICIT). pp. 2195–2199 (2006)
115. Mahapatra, D., Roy, P., Sedai, S., Garnavi, R.: A cnn based neurobiology inspired approach for retinal image quality assessment. In: In Proc. EMBC. pp. 1304–1307 (2016)
116. Mahapatra, D., Roy, P., Sedai, S., Garnavi, R.: Retinal image quality classification using saliency maps and cnns. In: In Proc. MICCAI-MLMI. pp. 172–179 (2016)
117. Mahapatra, D., Roy, S., Sun, Y.: Retrieval of mr kidney images by incorporating shape information in histogram of low level features. In: In 13th International Conference on Biomedical Engineering. pp. 661–664 (2009)
118. Mahapatra, D., Saha, S., Vishwanath, A., Bastide, P.: Generating hyperspectral image database by machine learning and mapping of color images to hyperspectral domain. In: US Patent App. 15/949,528 (2019)
119. Mahapatra, D., Saini, M.: A particle filter framework for object tracking using visual-saliency information. *Intelligent Multimedia Surveillance* pp. 133–147 (2013)
120. Mahapatra, D., Saini, M., Sun, Y.: Illumination invariant tracking in office environments using neurobiology-saliency based particle filter. In: IEEE ICME. pp. 953–956 (2008)
121. Mahapatra, D., Schüffler, P., Tielbeek, J., Vos, F., Buhmann, J.: Semi-supervised and active learning for automatic segmentation of crohn's disease. In: Proc. MICCAI, Part 2. pp. 214–221 (2013)
122. Mahapatra, D., Sedai, S., Garnavi, R.: Elastic registration of medical images with gans. In: arXiv preprint arXiv:1805.02369 (2018)
123. Mahapatra, D., Sedai, S., Halupka, K.: Uncertainty region based image enhancement. In: US Patent App. 10,832,074 (2020)
124. Mahapatra, D., Singh, A.: Ct image synthesis using weakly supervised segmentation and geometric inter-label relations for covid image analysis. In: arXiv preprint arXiv:2106.10230 (2021)
125. Mahapatra, D., Sun, Y.: Nonrigid registration of dynamic renal MR images using a saliency based MRF model. In: Proc. MICCAI. pp. 771–779 (2008)
126. Mahapatra, D., Sun, Y.: Registration of dynamic renal mr images using neurobiological model of saliency. In: Proc. ISBI. pp. 1119–1122 (2008)
127. Mahapatra, D., Sun, Y.: Using saliency features for graphcut segmentation of perfusion kidney images. In: In 13th International Conference on Biomedical Engineering (2008)

128. Mahapatra, D., Sun, Y.: Joint registration and segmentation of dynamic cardiac perfusion images using mrf. In: Proc. MICCAI. pp. 493–501 (2010)
129. Mahapatra, D., Sun, Y.: Mrf based joint registration and segmentation of dynamic renal mr images. In: Second International Conference on Digital Image Processing. vol. 7546, pp. 285–290 (2010)
130. Mahapatra, D., Sun, Y.: An mrf framework for joint registration and segmentation of natural and perfusion images. In: Proc. IEEE ICIP. pp. 1709–1712 (2010)
131. Mahapatra, D., Sun, Y.: Retrieval of perfusion images using cosegmentation and shape context information. In: Proc. APSIPA Annual Summit and Conference (ASC). vol. 35 (2010)
132. Mahapatra, D., Sun, Y.: Rigid registration of renal perfusion images using a neurobiology based visual saliency model. EURASIP Journal on Image and Video Processing. pp. 1–16 (2010)
133. Mahapatra, D., Sun, Y.: Mrf based intensity invariant elastic registration of cardiac perfusion images using saliency information. IEEE Trans. Biomed. Engg. **58**(4), 991–1000 (2011)
134. Mahapatra, D., Sun, Y.: Orientation histograms as shape priors for left ventricle segmentation using graph cuts. In: In Proc: MICCAI. pp. 420–427 (2011)
135. Mahapatra, D., Sun, Y.: Integrating segmentation information for improved mrf-based elastic image registration. IEEE Trans. Imag. Proc. **21**(1), 170–183 (2012)
136. Mahapatra, D., Tielbeek, J., Buhmann, J., Vos, F.: A supervised learning based approach to detect crohn’s disease in abdominal mr volumes. In: Proc. MICCAI workshop Computational and Clinical Applications in Abdominal Imaging(MICCAI-ABD). pp. 97–106 (2012)
137. Mahapatra, D., Tielbeek, J., Vos, F., ., J.B.: Crohn’s disease tissue segmentation from abdominal mri using semantic information and graph cuts. In: Proc. IEEE ISBI. pp. 358–361 (2013)
138. Mahapatra, D., Tielbeek, J., Vos, F., Buhmann, J.: Localizing and segmenting crohn’s disease affected regions in abdominal mri using novel context features. In: Proc. SPIE Medical Imaging (2013)
139. Mahapatra, D., Tielbeek, J., Vos, F., Buhmann, J.: Weakly supervised semantic segmentation of crohn’s disease tissues from abdominal mri. In: Proc. IEEE ISBI. pp. 832–835 (2013)
140. Mahapatra, D., Vos, F., Buhmann, J.: Crohn’s disease segmentation from mri using learned image priors. In: In Proc. IEEE ISBI. pp. 625–628 (2015)
141. Mahapatra, D., Vos, F., Buhmann, J.: Active learning based segmentation of crohns disease from abdominal mri. Computer Methods and Programs in Biomedicine **128**(1), 75–85 (2016)
142. Mahapatra, D., Winkler, S., Yen, S.: Motion saliency outweighs other low-level features while watching videos. In: SPIE HVEI. pp. 1–10 (2008)
143. Mahapatra, D.: Registration and segmentation methodology for perfusion mr images: Application to cardiac and renal images. - pp. - (2011)
144. Mahapatra, D.: Registration and segmentation methodology for perfusion mr images: Application to cardiac and renal images. - pp. - (2011)
145. Mahapatra, D.: Multimodal generalized zero shot learning for gleason grading using self-supervised learning. In: arXiv preprint arXiv:2111.07646 (2021)
146. Mahapatra, D., Ge, Z.: MR image super resolution by combining feature disentanglement CNNs and vision transformers. In: Medical Imaging with Deep Learning (2022)
147. Mahapatra, D., Ge, Z.: Mr image super resolution by combining feature disentanglement cnns and vision transformers. In: - (2022)

148. Mahapatra, D., Ge, Z.: Mr image super resolution by combining feature disentanglement cnns and vision transformers. In: - (2022)
149. Mahapatra, D., Ge, Z., Reyes, M.: Self-supervised generalized zero shot learning for medical image classification using novel interpretable saliency maps. *IEEE Transactions on Medical Imaging* pp. 1–1 (2022). <https://doi.org/10.1109/TMI.2022.3163232>
150. Mahapatra, D., Korevaar, S., Tennakoon, R.: Gcn based unsupervised domain adaptation with feature disentanglement for medical image classification. In: - (2022)
151. Mahapatra, D., Poellinger, A., Shao, L., Reyes, M.: Interpretability-driven sample selection using self supervised learning for disease classification and segmentation. *IEEE TMI* pp. 1–15 (2021)
152. Motiian, S., Jones, Q., et al.: Few-shot adversarial domain adaptation. In: *Proc. NeurIPS*. p. 6673–6683 (2017)
153. Ouyang, C., Kamnitsas, K., et al.: Data efficient unsupervised domain adaptation for cross-modality image segmentation. In: *MICCAI*. p. 669–677 (2019)
154. Painchaud, N., Skandarani, Y., et al.: Cardiac segmentation with strong anatomical guarantees. *IEEE Trans. Med. Imag.* **39**(11), 3703–3713 (2020)
155. Pandey, A., Paliwal, B., Dhall, A., Subramanian, R., Mahapatra, D.: This explains that: Congruent image–report generation for explainable medical image analysis with cyclic generative adversarial networks. In: *In MICCAI-iMIMIC 2021*. pp. 1–11 (2021)
156. Park, T., Zhu, J.Y., Wang, O., Lu, J., Shechtman, E., Efros, A.A., Zhang, R.: Swapping autoencoder for deep image manipulation. In: *Advances in Neural Information Processing Systems* (2020)
157. Puybareau, É., Zhao, Z., et al.: Left atrial segmentation in a few seconds using fully convolutional network and transfer learning. In: *STACOM Atrial Segmentation and LV Quantification Challenges*. pp. 339–347 (2019)
158. Rajpurkar, P., Irvin, J., et al.: Chexnet: Radiologist-level pneumonia detection on chest x-rays with deep learning. In: *arXiv preprint arXiv:1711.05225*, (2017)
159. Roy, P., Chakravorty, R., Sedai, S., Mahapatra, D., Garnavi, R.: Automatic eye type detection in retinal fundus image using fusion of transfer learning and anatomical features. In: *In Proc. DICTA*. pp. 1–7 (2016)
160. Roy, P., Tennakoon, R., Cao, K., Sedai, S., Mahapatra, D., Maetschke, S., Garnavi, R.: A novel hybrid approach for severity assessment of diabetic retinopathy in colour fundus images,. In: *In Proc. IEEE ISBI*. pp. 1078–1082 (2017)
161. Roy, P., Mahapatra, D., Garnavi, R., Tennakoon, R.: System and method to teach and evaluate image grading performance using prior learned expert knowledge base. In: *US Patent App. 10,984,674* (2021)
162. Saini, M., Guthier, B., Kuang, H., Mahapatra, D., Saddik, A.: szoom: A framework for automatic zoom into high resolution surveillance videos. In: *arXiv preprint arXiv:1909.10164* (2019)
163. Schüffler, P., Mahapatra, D., Tielbeek, J., Vos, F., Makanyanga, J., Pends, D., Nio, C., Stoker, J., Taylor, S., Buhmann, J.: A model development pipeline for crohns disease severity assessment from magnetic resonance images. In: *In Proc: MICCAI-ABD* (2013)
164. Schüffler, P., Mahapatra, D., Tielbeek, J., Vos, F., Makanyanga, J., Pends, D., Nio, C., Stoker, J., Taylor, S., Buhmann, J.: Semi automatic crohns disease severity assessment on mr imaging. In: *In Proc: MICCAI-ABD* (2014)

165. Schüffler, P.J., Mahapatra, D., Vos, F.M., Buhmann, J.M.: Computer aided crohn's disease severity assessment in mri. In: VIGOR++ Workshop 2014- Showcase of Research Outcomes and Future Outlook. pp. – (2014)
166. Sedai, S., Mahapatra, D., Antony, B., Garnavi, R.: Joint segmentation and uncertainty visualization of retinal layers in optical coherence tomography images using bayesian deep learning. In: In Proc. MICCAI-OMIA. pp. 219–227 (2018)
167. Sedai, S., Mahapatra, D., Ge, Z., Chakravorty, R., Garnavi, R.: Deep multiscale convolutional feature learning for weakly supervised localization of chest pathologies in x-ray images. In: In Proc. MICCAI-MLMI. pp. 267–275 (2018)
168. Sedai, S., Mahapatra, D., Hewavitharanage, S., Maetschke, S., Garnavi, R.: Semi-supervised segmentation of optic cup in retinal fundus images using variational autoencoder,. In: In Proc. MICCAI. pp. 75–82 (2017)
169. Sedai, S., Roy, P., Mahapatra, D., Garnavi, R.: Segmentation of optic disc and optic cup in retinal fundus images using shape regression. In: In Proc. EMBC. pp. 3260–3264 (2016)
170. Sedai, S., Roy, P., Mahapatra, D., Garnavi, R.: Segmentation of optic disc and optic cup in retinal images using coupled shape regression. In: In Proc. MICCAI-OMIA. pp. 1–8 (2016)
171. Srivastava, S., Yaqub, M., Nandakumar, K., Ge, Z., Mahapatra, D.: Continual domain incremental learning for chest x-ray classification in low-resource clinical settings. In: In MICCAI-FAIR 2021. pp. 1–11 (2021)
172. Tennakoon, R., Mahapatra, D., Roy, P., Sedai, S., Garnavi, R.: Image quality classification for dr screening using convolutional neural networks. In: In Proc. MICCAI-OMIA. pp. 113–120 (2016)
173. Tong, J., Mahapatra, D., Bonnington, P., Drummond, T., Ge, Z.: Registration of histopathology images using self supervised fine grained feature maps. In: In Proc. MICCAI-DART Workshop. pp. 41–51 (2020)
174. Vahadane, A., Peng, T., et al.: Structure-preserving color normalization and sparse stain separation for histological images. *IEEE Trans. Med. Imag.* **35**(8), 1962–1971 (2016)
175. Verma, R., Kumar, N., Patil, A., Kurian, N.C., Rane, S., Graham, S., Vu, Q.D., Zwager, M., Raza, S.E.A., Rajpoot, N., Wu, X., Chen, H., Huang, Y., Wang, L., Jung, H., Brown, G.T., Liu, Y., Liu, S., Jahromi, S.A.F., Khani, A.A., Montahaei, E., Baghshah, M.S., Behroozi, H., Semkin, P., Rassadin, A., Dutande, P., Lodaya, R., Baid, U., Baheti, B., Talbar, S., Mahbod, A., Ecker, R., Ellinger, I., Luo, Z., Dong, B., Xu, Z., Yao, Y., Lv, S., Feng, M., Xu, K., Zunair, H., Hamza, A.B., Smiley, S., Yin, T.K., Fang, Q.R., Srivastava, S., Mahapatra, D., Trnavska, L., Zhang, H., Narayanan, P.L., Law, J., Yuan, Y., Tejomay, A., Mitkari, A., Koka, D., Ramachandra, V., Kini, L., Sethi, A.: Monusac2020: A multi-organ nuclei segmentation and classification challenge. *IEEE Transactions on Medical Imaging* **40**(12), 3413–3423 (2021). <https://doi.org/10.1109/TMI.2021.3085712>
176. Vos, F.M., Tielbeek, J., Naziroglu, R., Li, Z., Schüffler, P., Mahapatra, D., Wiebel, A., Lavini, C., Buhmann, J., Hege, H., Stoker, J., van Vliet, L.: Computational modeling for assessment of IBD: to be or not to be? In: Proc. IEEE EMBC. pp. 3974–3977 (2012)
177. Wang, X., Peng, Y., et al.: Chestx-ray8: Hospital-scale chest x-ray database and benchmarks on weakly-supervised classification and localization of common thorax diseases. In: In Proc. CVPR (2017)
178. Wu, M., Pan, S., Zhou, C., Chang, X., Zhu, X.: Unsupervised domain adaptive graph convolutional networks. In: Proceedings of The Web Conference 2020. pp. 1457–1467 (2020)

179. Xie, S., Zheng, Z., Chen, L., Chen, C.: Learning semantic representations for unsupervised domain adaptation. In: Proc. ICML. vol. 80, pp. 5423–5432 (2018)
180. Xing, Y., Ge, Z., Zeng, R., Mahapatra, D., Seah, J., Law, M., Drummond, T.: Adversarial pulmonary pathology translation for pairwise chest x-ray data augmentation. In: In Proc. MICCAI. pp. 757–765 (2019)
181. Zilly, J., Buhmann, J., Mahapatra, D.: Boosting convolutional filters with entropy sampling for optic cup and disc image segmentation from fundus images. In: In Proc. MLMI. pp. 136–143 (2015)
182. Zilly, J., Buhmann, J., Mahapatra, D.: Glaucoma detection using entropy sampling and ensemble learning for automatic optic cup and disc segmentation. In Press *Computerized Medical Imaging and Graphics* **55**(1), 28–41 (2017)